Inorganic Chemistry

Article

Eu(III) Complexes of Tetradentate Ligands Related to 2,9-Di(pyrid-2′-yl)-1,10-phenanthroline and 2,2′-Bi-1,10-phenanthroline

Ruifa Zong,[†] Gang Zhang,[†] Svetlana V. Eliseeva,[‡] Jean-Claude G. Bünzli,*,[‡] and Randolph P. Thummel*,[†]

[†]*Department of Chemistry, 136 Fleming Building, University of Houston, Houston, Texas 77204-5003, and* [‡]*Laboratory of Lanthanide Supramolecular Chemistry, Swiss Federal Institute of Technology, Lausanne (EPFL), Switzerland*

A series of six tetradentate polypyridine-type ligands (L) have been used to prepare the corresponding Eu(III) complexes $[Eu(L)_2(S)]^{n+}$ (n = 2, 3) where S = H_2O or $CF_3SO_3^-$. Two of the ligands, 2,9-di(pyrid-2′-yl)-1,10-phenanthroline (**4**) and its dipyridophenazine analogue (**6**) are symmetrical around a central phenanthroline ring. The other four ligands are 2,2′-bi-1,10-phenanthroline and its 3,3′-di-, tri-, and tetramethylene-bridged analogues (**5a-d**) whose conformations are governed by the length of the polymethylene bridge. ^{1}H NMR and X-ray analysis indicate that all of the complexes have a C_{2v} symmetry. The biphenanthroline series shows a strong correlation of the conjugation between the two halves of the ligand, as governed by the bridge, with the absorption and emission properties of the Eu(III) complex. The complex having the most distorted, tetramethylene-bridged ligand exhibits a weak, high energy $\pi-\pi^*$ absorption and low sensitization efficiency. The luminescence decays are monoexponential for complexes of **4** and either monoexponential or biexponential for the complexes of **5** depending on its solution concentration and the length of the bridge. The complexes of **4** exhibit much longer lifetime, higher overall quantum yield, and higher sensitization efficiency than complexes of **5** while the complex of **6** emits very weakly. The Eu($^5D_0$) lifetime for $[Eu(\mathbf{4})_2(H_2O)](ClO_4)_3$ is shorter than for $[Eu(\mathbf{4})_2(CF_3SO_3)](CF_3SO_3)_2$, reflecting the effect of the coordinated water. The complexes are examined for stability in the presence of water and found to retain most of their luminescent properties even in the presence of a large excess of water.

Introduction

Luminescent Eu(III) complexes show considerable promise as low energy emitters in a variety of applications.[1] For polypyridine ligand complexes, this luminescence involves the absorption of light by the ligand to form a singlet excited state followed by intersystem crossing to the triplet and then energy transfer to the metal center that then emits longer wavelength light. Ligands, such as the cryptands, which effectively protect the metal center from competing radiationless deactivation by surrounding solvent molecules, often lead to very impressive emission properties.[2] In earlier work, we attempted to complex several large polypyridine ligands with Eu(III) in an effort to accomplish similar protection of the metal.[3] However, we discovered that Eu(III) is quite demanding in the geometry that it will accommodate as its coordination sphere. As a nine-coordinate species, Eu(III) will accommodate three tridentate ligands such as 2,2′;6′,2″-terpyridine (**1**, tpy);[4] however complexes with this ligand are somewhat labile, being especially sensitive to the presence of water.[5] We discovered that bridging the tpy between the 3,3′ and 5′,3″ positions would hold it in a *syn,syn*-conformation

*To whom correspondence should be addressed. E-mail: thummel@uh.edu (R.P.T.), jean-claude.bunzli@epfl.ch (J.-C.G.B.).

(1) (a) Eliseeva, S. V.; Bünzli, J.-C. G. *Chem. Soc. Rev.* **2010**, *39*, 189–227. (b) Richardson, F. S. *Chem. Rev.* **1982**, *82*, 541–552. (c) Bünzli, J.-C. G. *Acc. Chem. Res.* **2006**, *39*, 53–61. (d) Song, B.; Wang, G.; Tan, M.; Yuan, J. *J. Am. Chem. Soc.* **2006**, *128*, 13442–13450. (e) Bünzli, J.-C. G.; Piguet, C. *Chem. Soc. Rev.* **2005**, *34*, 1048–1077. (f) Parker, D. *Chem. Soc. Rev.* **2004**, *33*, 156–165. (g) Piguet, C.; Edder, C.; Nozary, H.; Renaud, F.; Rigault, S.; Bünzli, J.-C. G. *J. Alloys Compd.* **2000**, *303–304*, 94–103. (h) Piguet, C.; Bünzli, J.-C. G. *Chem. Soc. Rev.* **1999**, *28*, 347–358. (i) Faulkner, S.; Matthews, J. L. In *Comprehensive coordination chemistry II*; McCleverty, J. A., Meyer, T. J., Eds.; Elsevier Pergamon : Amsterdam, Boston, 2004; Vol. 9, pp 913–944.

(2) (a) Sabbatini, N.; Guardigli, M.; Manet, I.; Ungaro, R.; Casnati, A.; Ziessel, R.; Ulrich, G.; Asfari, Z.; Lehn, J.-M. *Pure Appl. Chem.* **1995**, *67*, 135–140. (b) Alpha, B.; Lehn, J.-M.; Mathis, G. *Angew. Chem., Int. Ed. Engl.* **1987**, *26*, 266–267.

(3) Mallet, C.; Thummel, R. P.; Hery, C. *Inorg. Chim. Acta* **1993**, *210*, 223–231.

(4) (a) Durham, D. A.; Frost, G. H.; Hart, F. A. *J. Inorg. Nucl. Chem.* **1969**, *31*, 833–838. (b) Frost, G. H.; Hart, F. A.; Heath, C.; Hursthouse, M. B. *Chem. Commun.* **1969**, 1421–1422.

(5) Chapman, R. D.; Loda, R. T.; Riehl, J. P.; Schwartz, R. W. *Inorg. Chem.* **1984**, *23*, 1652–1657.

(**2**) thereby significantly improving the stability of its Eu complexes toward ligand replacement by water.[3,6]
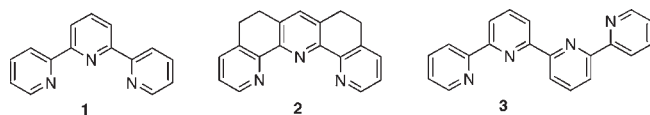
Ligands with higher denticity than tpy might form more robust complexes with the lanthanides. A well organized 2:1 complex is formed with 2,2′-bipyridine-6,6′-dicarboxylic acid but the ligand can also behave in a bridging fashion to provide a 2:3 metal/ligand stoichiometry.[7] Sexipyridine forms an unusual hexadentate complex with Eu(III).[8] There are two reports of a complex of Eu(III) with a tetradentate polypyridyl system, 6,6′-*bis*-(5,6-diethyl-[1,2,4]triazin-3-yl)-2,2′-bipyridine, where the ligand/metal ratio is a function of ligand concentration.[9] More often quaterpyridine (**3**) is found to be a bridging ligand[10] and it can also act as a tridentate ligand, forming ML_2 complexes with a dangling, uncomplexed pyridine.[11]

The substitution of a 1,10-phenanthroline (phen) subunit for one or two bpy subunits of quaterpyridine leads to 2,9-di(pyrid-2′-yl)phen (**4**) and 2,2′-biphen (**5a**). Quaterpyridine possesses three interpyridine bonds, leading to considerable conformational mobility. With only two or one such inter-pyridine bonds respectively, **4** and **5a** are less conformationally mobile and their coordination chemistry is thereby easier to predict and control. We have recently demonstrated that **4** will act as a tetradentate with Ru(II),[12] occupying the equatorial plane of the complex while **5a-d** will form a series of helical dinuclear complexes with Cu(I).[13]

The current study will demonstrate that these ligands will form well organized, relatively stable 2:1 complexes with Eu(III) in which the ninth coordination site is occupied by a single water molecule or the trifluoromethanesulfonate anion. The luminescence properties of these complexes are directly influenced by the nature of the tetradentate ligand.
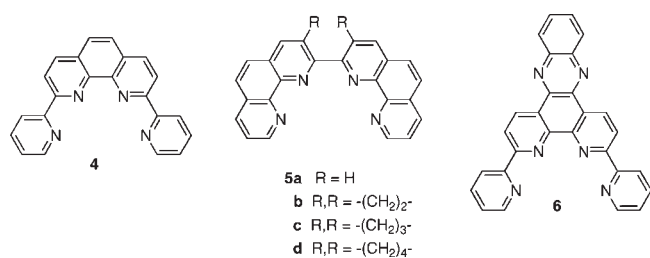
Results and Discussion

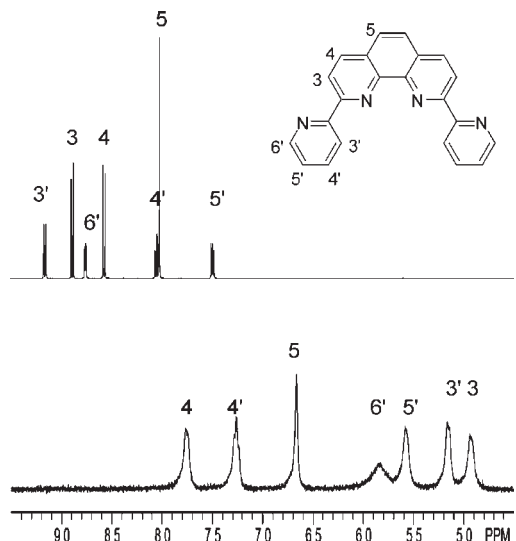In this study Eu(III) complexes were formed using the phen-containing ligands **4** and **5a-d** as well as the closely

Figure 1. ^{1}H NMR of **4** (top) and [Eu(**4**)₂(H₂O)](ClO₄)₃ (bottom) in acetone-d_6. Proton assignments made by 2D-COSY NMR.

related dipyridophenazine ligand **6**. The complexes were prepared by treating the ligand with an appropriate Eu(III) salt in refluxing methanol or ethanol and precipitating the product from the cooled solution. The complexes were analyzed by ^{1}H NMR, mass spectroscopy (MS), and combustion analysis. Having C_2 symmetry, the ligands showed relatively simple NMR spectra with 2 or 3 independent spin systems that were well resolved and could be easily assigned. Coordination with the paramagnetic Eu(III) ion caused the peaks to broaden and shift upfield (Figure 1). The poor resolution of the broadened peaks in the complexes prohibited their confident assignment in some cases. The important feature of these NMR spectra was their simplicity, strongly supporting a symmetrical bonding motif and a 2:1 ligand/metal ratio that was supported by the MS data. If the ligands had bound to Eu(III) in an unsymmetrical fashion their C_2 symmetry would have been destroyed, and the NMR spectrum would have shown at least twice as many resonances. It is interesting to note that an attempt to coordinate quaterpyridine **3** with Eu(III) was unsuccessful, leading to a mixture of unidentifiable products as well as unreacted ligand.

Definitive proof of structure was obtained by X-ray crystal analyses of the Eu(III) complexes of ligands **4** and **5b**. In the case of **4**, the complex was prepared as its perchlorate and trifluoromethanesulfonate salt. Because of the poor coordinating ability of the perchlorate anion and the presence of water in the reagent, this complex contained a water molecule in its ninth coordination site. For the complex of **5b**, when the counterion was anhydrous trifluoromethanesulfonate, this anion was also found to occupy the ninth coordination site. Two views of each of these structures are given in Figures 2

(6) Sénéchal-David, K.; Hemeryck, A.; Tancrez, N.; Toupet, L.; Williams, J. A. G.; Ledoux, I.; Zyss, J.; Boucekkine, A.; Guégan, J.-P.; Le Bozec, H.; Maury, O. *J. Am. Chem. Soc.* **2006**, *128*, 12243–12255.

(7) Bünzli, J.-C. G.; Charbonnière, L. J.; Ziessel, R. F. *J. Chem. Soc., Dalton Trans.* **2000**, 1917–1923.

(8) Constable, E. C.; Chotalia, R.; Tocher, D. A. *Chem. Commun.* **1992**, 771–773.

(9) (a) Drew, M. G. B.; Foreman, M. R. S. J.; Hill, C.; Hudson, M.; Madic, C. *Inorg. Chem. Commun.* **2005**, *8*, 239–241. (b) Trumm, S.; Lieser, G.; Foreman, M. R. S. J.; Panak, P. J.; Geist, A.; Fanghänel, T. *Dalton Trans.* **2010**, 923–929.

(10) Constable, E. C.; Cathey, C. J.; Hannon, M. J.; Tocher, D. A.; Walker, J. V.; Ward, M. D. *Polyhedron* **1999**, *18*, 159–173.

(11) (a) Dell' Amico, D. B.; Calderazzo, F.; Englert, U.; Labella, L.; Marchetti, F. *J. Chem. Soc., Dalton Trans.* **2001**, 357–358. (b) Dell' Amico, D. B.; Calderazzo, F.; Curiardi, M.; Labella, L.; Marchetti, F. *Inorg. Chem.* **2004**, *43*, 5459–5465.

(12) (a) Zong, R.; Thummel, R. P. *J. Am. Chem. Soc.* **2004**, *126*, 10800–10801. (b) Zhang, G.; Zong, R.; Tseng, H.-W.; Thummel, R. P. *Inorg. Chem.* **2008**, *47*, 990–998.

(13) Riesgo, E. C.; Hu, Y.-Z.; Thummel, R. P. *Inorg. Chem.* **2003**, *42*, 6648–6654.
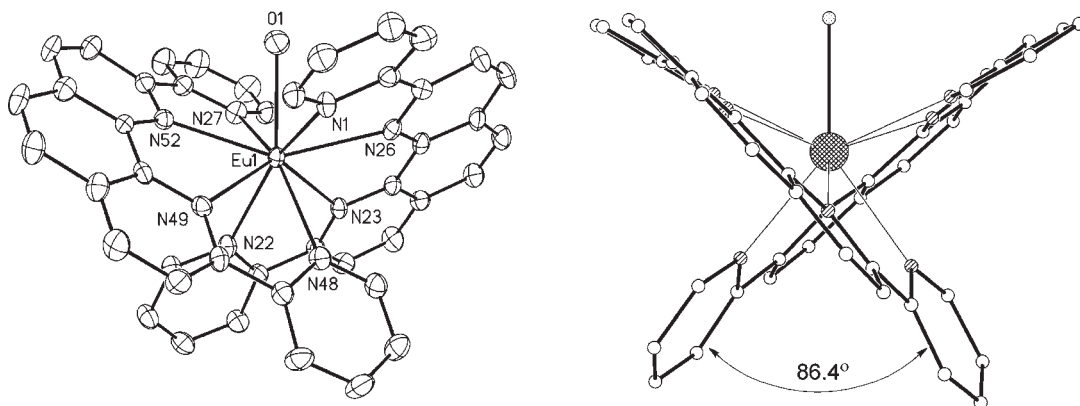
Figure 2. ORTEP plot of [Eu(**4**)$_2$(OH$_2$)]$^{3+}$ with the atom labeling scheme (left) as well as a view showing the two ligand planes and the Eu−OH$_2$ bond (right).
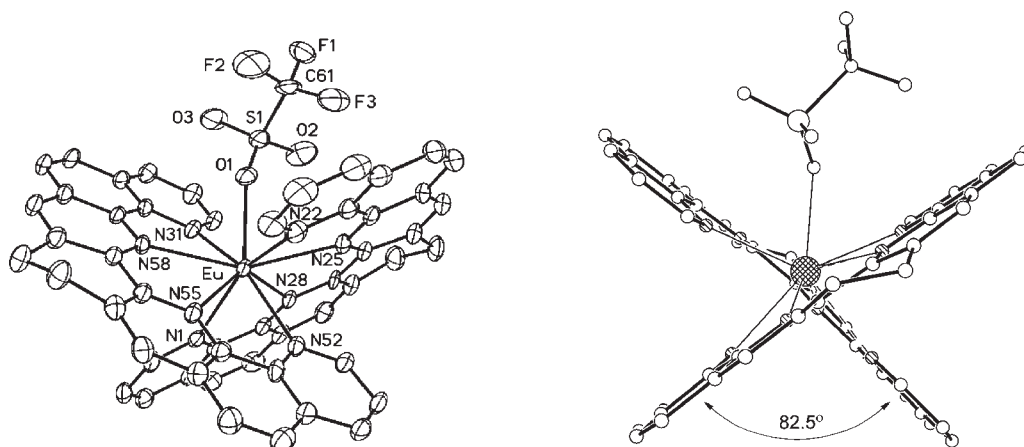
Figure 3. ORTEP plot of [Eu(**5b**)$_2$(OSO$_2$CF$_3$)]$^{2+}$ with the atom labeling scheme (left) as well as a view showing the two ligand planes and the Eu−O(triflate) bond (right).

and 3 and some pertinent geometric data are collected in Table 1. It is interesting to note that both crystals were grown from CH$_3$CN solution, indicating that Eu(III) shows a higher affinity for water or triflate than CH$_3$CN. Considering that crystal packing forces may have played a role, this observation can not exclude the possibility that the aquo or triflato ligands are being replaced by acetonitrile in solution.

For both structures the Eu−N bond lengths range from 2.52 to 2.67 Å. These bonds can be grouped into "inner" and "outer" bonds. The inner bonds involve the two nitrogens located nearest the central axis of the ligand and the outer bonds involve the peripheral nitrogens. The inner Eu−N bonds are shorter, ranging from 2.52 to 2.55 Å while the outer bonds are longer, up to 2.67 Å. It is interesting that the Eu is not symmetrically disposed between the two outer nitrogens, especially in the complex of **4** where one ligand shows outer bond lengths of 2.59 and 2.64 Å and the other shows 2.56 and 2.65 Å.

The ligands **4** and **5b** differ considerably in their extent of preorganization. The dipyridylphen **4** has two intraligand single bonds between the pyridine rings and the central phen, allowing for a certain amount of flexibility and conformational mobility. On the other hand, the biphen **5b** is more rigid with a relatively low, but significant, barrier to conformational inversion about the central 2,2′-bond. The coordination sphere of both complexes contains three fused five-membered chelate rings associated with each of the two

ligands. For the complex of **4**, the N−Eu−N angle of the central chelate ring is greater than for the two outer chelate rings, reflecting, to some extent, the flexibility of the phen-pyridine bonds. For the complex of the more rigid bridged biphen **5b** this effect is less apparent, reflecting less flexibility in the two outer phen rings. This same flexibility is also evidenced by the dihedral angles between the planes of adjacent pyridine rings. In the more flexible complex of **4** these angles are greater, up to 15.3°, than in the complex of **5b** where the largest dihedral angle is 4.7°. From the side-on view on the right side of Figures 2 and 3 it can be seen that the Eu(III) cation is slightly out of the plane of the two ligands. This effect is more pronounced for the more flexible ligand **4**. For both complexes the two ligands are nearly orthogonal and the dihedral angle between the mean planes of the two outermost pyridines is indicated in the figure, 86.4° for [Eu(**4**)$_2$(OH$_2$)]$^{3+}$ and 82.5° for [Eu(**5b**)$_2$(OSO$_2$CF$_3$)]$^{2+}$.

The electronic absorption spectra of the ligands and their Eu(III) complexes have been measured in CH$_3$CN for 2 × 10^{-5} M solutions to minimize intermolecular interactions, and the absorption data are assembled in Table 2. The lowest energy absorption band of the ligands is associated with a π−π* transition. The energy of this transition is dependent on both the electronegativity of the ligand as well as its π-electron delocalization. Thus ligand **6**, with a quinoxaline ring fused to the central ring of the phen portion of **4**, is both more electronegative and more delocalized, exhibiting a long

wavelength band at 393 nm as opposed to the higher energy absorption at 356 nm observed for **4**. For the series of biphen ligands **5a-d**, the dihedral angle about the central 2,2′-bond is controlled by the length of the 3,3′-polymethylene bridge. In earlier work we have estimated this angle to be 16° for **5b**, 44° for **5c**, and 60° for **5d**.[13] The larger the twist angle between the two phen rings, the less interacting are their π-systems and thus the higher energy (shorter wavelength) is their absorption: 343 nm for **5d** versus 377 nm for **5b** with **5c** intermediate at 353 nm. The intensity of these absorption bands also follows the same trend with the most planar ligand **5b** showing the most intense absorption (Figure 4-top). The unbridged system **5a** shows a long wavelength band at 366 nm suggesting a dihedral angle somewhere between **5b** and **5c**. It should be pointed out, however, that **5a** most likely

exists in a transoid conformation so that it is not readily comparable to its cisoid bridged analogues.

Although the ligand conformations are certainly modulated by Eu(III) complexation, the observed effects are consistent with the longest wavelength band being associated with a $\pi-\pi^*$ absorption of the metal-bound ligand. Figure 4 (bottom) shows a nice progression for this long wavelength band along the series of Eu(III) complexes of **5b**, **5c**, and **5d**. For the complex of the unbridged biphen **5a**, the ligand is

Table 1. Selected Structural Data for $[Eu(4)_2(OH_2)]^{3+}$ and $[Eu(5b)_2(CF_3SO_3)]^{2+\,a}$

$[Eu(4)(OH_2)]^{3+b}$		$[Eu(5b)(CF_3SO_3)]^{3+}$	
Bond Lengths (Å)			
Eu−N27	2.640(6)	Eu−N31	2.668(4)
Eu−N52	2.530(5)	Eu−N58	2.545(4)
Eu−N49	2.538(5)	Eu−N55	2.526(5)
Eu−N48	2.586(6)	Eu−N52	2.581(5)
Eu−N22	2.560(6)	Eu−N22	2.635(5)
Eu−N23	2.529(5)	Eu−N25	2.526(5)
Eu−N26	2.543(5)	Eu−N28	2.522(4)
Eu−N1	2.653(6)	Eu−N1	2.600(5)
Bond Angles (deg)			
N27−Eu−N52	63.16(17)	N31−Eu−N58	63.75(14)
N52−Eu−N49	64.05(17)	N58−Eu−N55	62.91(14)
N49−Eu−N48	63.01(17)	N55−Eu−N52	64.29(15)
N1−Eu−N26	62.81(16)	N22−Eu−N25	64.17(16)
N26−Eu−N23	64.10(17)	N25−Eu−N28	63.86(15)
N23−Eu−N22	63.78(17)	N28−Eu−N1	63.81(15)
N27−Eu−N48	148.3	N31−Eu−N52	149.1
N1−Eu−N22	149.45	N22−Eu−N1	149.2
O−Eu−N27	66.60(18)	N1−Eu−O	69.9(2)
N1−Eu−O	67.59(18)	O−Eu−N22	65.5(2)
Dihedral Angles (deg)			
N49−C42−C−43−N48	15.3(9)	N52−C53−C54−N55	4.6(8)
N49−C50−C51−N52	3.6(9)	N55−C56−C57−N58	−4.7(8)
N27−C32−C33−N52	−11.5(9)	N58−C59−C60−N31	1.3(8)
N23−C16−C17−N22	12.7(9)	N22−C23−C24−N25	−0.1(8)
N23−C24−C25−N26	2.4(9)	N25−C26−C−27−N28	−3.9(7)
N1−C6−C7−N26	−6.5(9)	N28−C29−C30−N1	0.4(7)

^{a} Atom numbering scheme in Figures 2 and 3. ^{b} Data is reported for one of the two cations in the unit cell.

Figure 4. Electronic absorption spectra: top: Ligands **L**; bottom: $[Eu(L)_2(CF_3SO_3)]^{2+}$ in CH_3CN (2.0 × 10^{-5} M); **L = 5a**, (black); **L = 5b**, (red); **L = 5c**, (green); **L = 5d**, (blue).

Table 2. Absorption Maxima of Ligands **4−6** and $[Eu(4−6)_2(CF_3SO_3)](CF_3SO_3)_2{}^a$

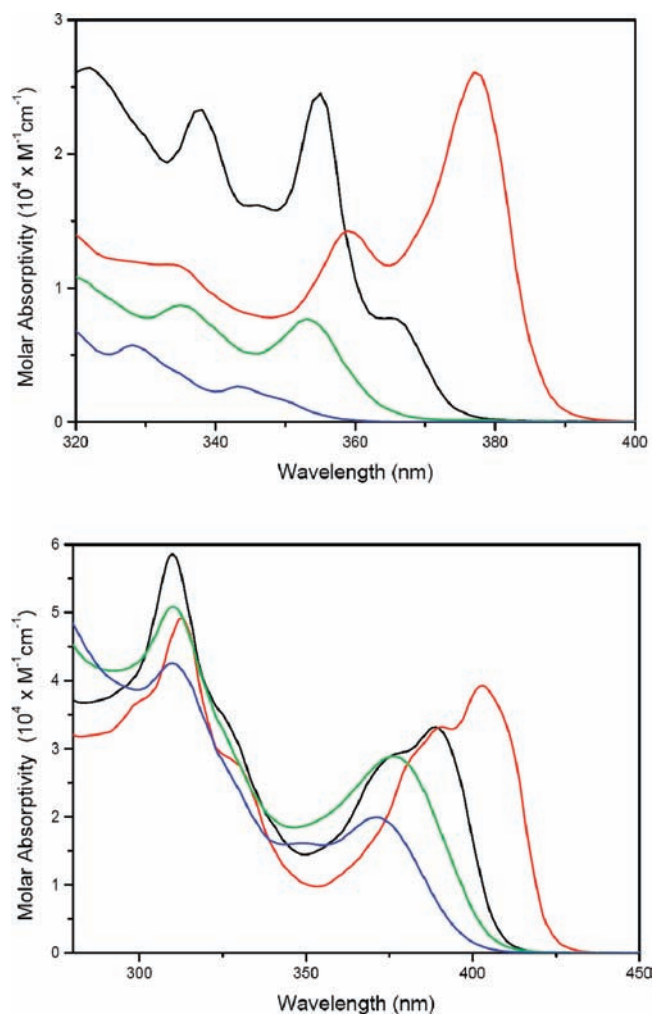| compound	λ, nm (log ε)
4	247(4.61), 287(4.56), 298(sh, 4.48), 303(sh, 4.46), 326(4.38), 341(4.27), 356(sh, 3.66)
5a	237(4.75), 262(4.37), 293(4.53), 322(4.42), 338(4.37), 355(4.39), 366(sh, 3.89)
5b	235(4.68), 264(4.50), 304(4.35), 334(sh, 4.07), 359(4.15), 377(4.42)
5c	236(4.59), 265(4.39), 293(4.28), 320(sh, 4.03), 335(3.94), 353(3.89)
5d	234(4.79), 267(4.62), 279(sh, 4.59), 328(3.76), 343(3.43)
6	294(4.63), 314(4.55), 326(4.54), 354(4.03), 373(4.13), 393(4.16)
$[Eu(4)_2]^{3+}$	241(4.69), 269(sh, 4.67), 279(4.71), 287(4.72), 333(4.64)
$[Eu(5a)_2]^{3+}$	227(4.97), 263(4.75), 310(4.77), 378(sh, 4.47), 389(4.52)
$[Eu(5b)_2]^{3+}$	233(4.95), 267(4.72), 302(sh, 4.57), 313(4.69), 326(4.46), 391(4.52), 403(4.59)
$[Eu(5c)_2]^{3+}$	240(4.95), 267(4.76), 310(4.71), 376(4.46)
$[Eu(5d)_2]^{3+}$	237(4.86), 273(4.71), 310(4.63), 349(4.20), 371(4.30)
$[Eu(6)_2]^{3+}$	213(4.65), 243(4.42), 303(4.69), 337(4.65), 366(sh, 4.45), 390 (4.05)

^{a} In 2.0 × 10^{-5} M CH_3CN at 20 °C.

Table 3. Photophysical Parameters Measured for Europium Complexes in the Solid State

compound	τ_{obs}, ms^{a,b}	τ_{rad}, ms^{c,d}	Q_{Eu}^{Eu}, %^{c}	Q_{Ln}^{L}, %^{b,c}	η_{sens}, %^{c}
Eu(**1**)$_3$(ClO$_4$)$_3$	1.95(2)	5.73	34	43(1)	∼100(15)
Eu(**4**)$_2$(ClO$_4$)$_3$(H$_2$O)	0.53(1)	3.75	14	15.5(3)	∼100(15)
Eu(**4**)$_2$(CF$_3$SO$_3$)$_3$	1.45(4)	3.49	42	29.8(5)	71(11)
Eu(**5a**)$_2$(CF$_3$SO$_3$)$_3$	0.043(1)	3.49	1.2	1.4(1)	∼100(15)
Eu(**5b**)$_2$(CF$_3$SO$_3$)$_3$	0.013(1)	3.64	0.36	0.37(4)	∼100(15)
Eu(**5c**)$_2$(CF$_3$SO$_3$)$_3$	0.074(2) (91%) 0.014(1) (9%) $\langle\tau\rangle = 0.073^e$	3.36	2.2	1.2(1)	55(8)
Eu(**5d**)$_2$(CF$_3$SO$_3$)$_3$	0.33(4) (60%) 0.10(2) (40%) $\langle\tau\rangle = 0.29^e$	3.27	8.9	3.8(1)	43(6)
Eu(**6**)$_2$(CF$_3$SO$_3$)$_3$	$9.3(2) \times 10^{-4}$	2.72	0.034	$3.0(5) \times 10^{-3}$	11(2)

^{a} Measured under laser excitation at 355 nm. ^{b} In parentheses: (2σ) values for three measurements. ^{c} See ref 1a for definitions and relevant equations. ^{d} Refractive index taken as being equal to 1.5 (see ref 14) $^e \langle\tau\rangle = \sum_i B_i \tau_i^2 / \sum_i B_i \tau_i$.

Table 4. Photophysical Parameters for Europium Complexes in CH$_3$CN

compound	c/M	τ_{obs}, ms^{a,b}	τ_{rad}, ms^c	Q_{Eu}^{Eu}, %^{d}	Q_{Ln}^{L} %^{b,e}	η_{sens}, %
Eu(**1**)$_3$(ClO$_4$)$_3$	10^{-4}	2.15(4)	6.17	35	28.8(1)	82(12)
	10^{-3}	2.34(2)	6.75	35	29.3(2)	84(12)
Eu(**4**)$_2$(ClO$_4$)$_3$(H$_2$O)	10^{-4}	1.65(2)	4.53	36	33.2(7)	92(14)
	10^{-3}	1.55(4)	4.77	32	29.0(3)	91(14)
Eu(**4**)$_2$(CF$_3$SO$_3$)$_3$	10^{-4}	1.85(1)	4.56	41	36.8(1)	90(14)
	10^{-3}	2.13(4)	4.67	46	39.3(1)	85(13)
Eu(**5a**)$_2$(CF$_3$SO$_3$)$_3$	10^{-4}	0.27(1) (88%) 0.083(1) (12%) $\langle\tau\rangle = 0.26^f$	4.31	6.0	3.7(1)	62(9)
	10^{-3}	0.28(2) (41%) 0.088(2) (59%) $\langle\tau\rangle = 0.22^f$	4.38	5.0	2.4(1)	48(7)
Eu(**5b**)$_2$(CF$_3$SO$_3$)$_3$	10^{-4}	0.14(2) (40%) 0.050(2) (60%) $\langle\tau\rangle = 0.11^f$	3.92	3.0	1.2(1)	40(6)
	10^{-3}	0.064(1) (47%) 0.019(1) (53%) $\langle\tau\rangle = 0.053^f$	3.97	1.3	0.63(5)	48(7)
Eu(**5c**)$_2$(CF$_3$SO$_3$)$_3$	10^{-4}	0.51(2)	3.69	14	12.4(7)	89(13)
	10^{-3}	0.59(2) (75%) 0.062(1) (25%) $\langle\tau\rangle = 0.57^f$	3.77	15	4.3(3)	29(4)
Eu(**5d**)$_2$(CF$_3$SO$_3$)$_3$	10^{-4}	0.61(1)	3.67	17	12.8(4)	75(11)
	10^{-3}	0.67(2) (65%) 0.051(2) (35%) $\langle\tau\rangle = 0.65^f$	3.70	18	2.9(1)	16(2)
Eu(**6**)$_2$(CF$_3$SO$_3$)$_3$	2×10^{-5}	g	3.62	n.a.	$7.2(8) \times 10^{-3}$	n.a.

^{a} Measured under laser excitation at 355 nm. ^{b} In parentheses: (2σ) values for three measurements; accuracy is ± 10%. ^{c} Refractive index taken as equal to that of the neat solvent, 1.344. ^{d} Whenever relevant, based on $\langle\tau\rangle$ ^{e} Quantum yields were measured under excitation at 330 nm for samples Eu(**1**)$_3$(ClO$_4$)$_3$, Eu(**4**)$_2$(ClO$_4$)$_3$(H$_2$O), Eu(**4**)$_2$(CF$_3$SO$_3$)$_3$ and Eu(**6**)$_2$(CF$_3$SO$_3$)$_3$ or at 370 nm for the others. $^f \langle\tau\rangle = \sum_i B_i \tau_i^2 / \sum_i B_i \tau_i$. ^{g} Too low signal to be measured.

constrained to a cisoid conformation and thus it fits nicely between the dimethylene and trimethylene-bridged complexes. Like the energies of these bands, their intensities also reflect closely the intensity of the unbound ligand absorbances.

The emission from Eu(III) complexes is derived from sensitization of the lanthanide excited state by energy transfer from the ligand triplet. Since this emission is metal-based, the energies of the emission bands remain mostly invariant while differences are noted in their intensities. Photophysical properties were determined for solid state samples (Table 3) and for 10^{-3} and 10^{-4} M CH$_3$CN solutions (Table 4) under ligand excitation. Somewhat more concentrated solutions were used for emission than for absorption to provide better comparison with the solid state data and to avoid possible dissociation under more dilute conditions. The solid state spectra for the complexes of **5a-d** are depicted in Figure 5.

The sharp emissions are due to Eu(III) centered transitions $^5D_0 \rightarrow {}^7F_J$ ($J = 0-4$). The intense emissions from the Eu(III) center indicate effective sensitization of the metal by the tetradentate ligands. The dimethylene bridged complex of **5b** shows the weakest emission while the tetramethylene bridged complex of **5d** shows the strongest emission. The sensitization efficiency therefore depends on the length of the polymethylene bridge which affects the twist angle and the degree of conjugation between the two phen halves of **5**. The complex of the unbridged biphen **5a** shows behavior intermediate between that of **5c** and **5d**, which is different from the absorption behavior where the complex of **5a** is intermediate between **5b** and **5c**.

In considering the solid state data (Table 3), the Eu($^5D_0$) lifetime for Eu(**4**)$_2$(CF$_3$SO$_3$)$_3$ is larger than for Eu(**4**)$_2$-(ClO$_4$)$_3$(H$_2$O), reflecting the coordination of one water molecule in the inner coordination sphere of the latter
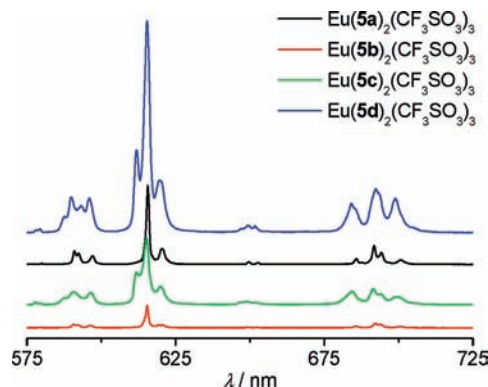
Figure 5. Solid state emission spectra: intensities are relative to Eu(**5a**)$_2$-(CF$_3$SO$_3$)$_3$ and scaled according to overall quantum yields.

Figure 6. Solid state emission spectra: intensities are relative to Eu(**4**)$_2$-(CF$_3$SO$_3$)$_3$ and scaled according to overall quantum yields.

complex. The luminescence decays for complexes with **5c** and **5d** are biexponential because of the presence of two distinct environments for the metal ion. For the complexes with ligands **5**, all lifetimes are very short. Since it is unlikely that the inner coordination sphere contains more than 2 bound water molecules, we may tentatively associate this short lifetime to the presence of a temperature-dependent non-radiative deactivation pathway.

For the solution emission data (Table 4), the parameters for the reference compound [Eu(**1**)$_3$(ClO$_4$)$_3$] compare well with those previously published: τ_{obs} = 2.31 ms and Q_{Ln}^{L} = 32%.[15]

The luminescence decays are monoexponential for the complexes with **4** but biexponential for the 10^{-3} M solutions of the complexes with ligands **5**, reflecting the presence of two species in solution. Upon dilution to 10^{-4} M they become monoexponential for ligands **5c** and **5d**, consistent with the presence of one major species in solution. The same observation as for the solid state samples applies in that these lifetimes are quite short for the complexes with ligands **5**, and these values cannot be entirely rationalized by considering potential binding of water molecules. Roughly speaking, one expects a ≈40% increase from the solid state values for radiative lifetimes if the coordination environment remains the same. This is not the case, particularly for the complexes with **5**.

The intrinsic quantum yield Q_{Eu}^{Eu} reflects the importance of non-radiative deactivations taking place in the surroundings of the metal ion (inner and outer coordination spheres). It amounts to 35–45% for complexes with **1** and **4**. Compared to solid state data, the constancy of Q_{Eu}^{Eu} between Eu(**4**)$_2$-(CF$_3$SO$_3$)$_3$ and Eu(**4**)$_2$(ClO$_4$)$_3$(H$_2$O) points to the water molecule being dissociated in acetonitrile solution. Q_{Eu}^{Eu} is much smaller for the complexes with ligands **5**, in line with the above comments. The overall quantum yields for the anhydrous complex with **4** and the solutions of the two, hydrated and anhydrous, complexes are the same and sizable (30–40%) consistent with a large sensitization efficiency (70–90%). Again these values are much smaller for the complexes with ligands **5**. Looking at the influence of the
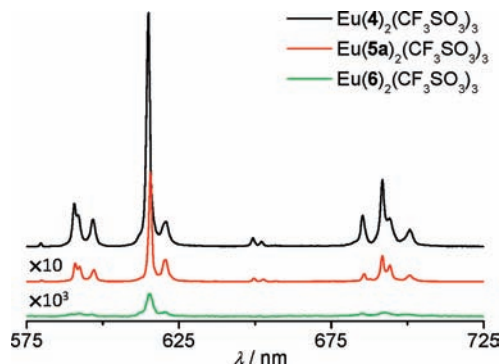
bridge, we note the following sequence for the overall quantum yields: **5d** > **5c** > **5a** > **5b** for solid state samples, **5c** > **5d** > **5a** > **5b** for 10^{-3} M solutions, and **5d** ≈ **5c** > **5a** > **5b** for 10^{-4} M solutions. However, when it comes to the sensitization efficiency of the ligands, the order is **5a** ≈ **5b** > **5c** > **5d** for solid state samples and for the more concentrated solution samples.

The Eu(III) complexes of **4**, **5a**, and **6** emit quite differently (Figure 6). The most delocalized system, involving ligand **6**, shows very weak emission while the system involving ligand **4**, with the highest energy π−π* transition, shows the strongest emission. The dimethylene-bridged biphen system shows intermediate behavior but is still fairly strongly emitting.

Water is a typical luminescence quencher of lanthanide excited states[16] as demonstrated by the shorter lifetime for Eu(**4**)$_2$(ClO$_4$)$_3$(H$_2$O) versus Eu(**4**)$_2$(CF$_3$SO$_3$)$_3$. Radiationless energy transfer competes with the radiative processes through coupling of the emissive states to the O-H vibrational overtones of coordinated water molecules.[17] In our earlier study on the stability of [Eu(tpy)$_3$]$^{3+}$ type complexes toward ligand replacement by water, we verified that the substitution of tpy was relatively facile[3] leading to complete quenching of the Eu(III) emission.

The incorporation of 3,3′-bridges between adjacent pyridine rings of tpy preorganized the ligand into a cisoid geometry and greatly increased stability of the system toward hydration.

The ligand **5b** possesses the quaterpyridine core with one ethano- and two etheno-bridges. It became of interest to determine whether the Eu(III) complex of such a ligand would show greater stability toward hydration. The bistetradentate complex is more "open" than the tris-tridentate one and from the right side views of Figures 2 and 3, one can see that three quadrants of the complex might be accessible for attack by water. A study on the effect of hydration on the luminescence was carried out by adding water to [Eu(**5b**)$_2$(CF$_3$SO$_3$)]$^{2+}$ 1 mM in degassed CH$_3$CN, keeping the complex concentration constant. The final water concentration was 18.5 M, corresponding to [H$_2$O]:[Eu] = 18′500. The corresponding changes induced in the emission spectra are shown in Figure 7.

(14) Shavaleev, N. M.; Eliseeva, S. V.; Scopelliti, R.; Bünzli, J.-C. G. *Chem. Eur. J.* **2009**, *15*, 10790–10802.

(15) Piguet, C.; Bünzli, J.-C. G. Self-assembled Lanthanide Helicates: from Basic Thermodynamics to Applications. In *Handbook on the Physics and Chemistry of Rare Earths*; Gschneidner, K. A., Jr., Bünzli, J.-C. G., Pecharsky, V. K., Eds.; Elsevier Science, B.V.: Amsterdam, 2010; Vol. *40*, Chapter 247, pp 351–553.

(16) (a) Supkowski, R. M.; Horrocks, W. D., Jr. *Inorg. Chim. Acta* **2002**, *430*, 44–48. (b) Pandya, S.; Yu, J.; Parker, D. *J. Chem. Soc., Dalton Trans.* **2006**, 2757–2766.

(17) (a) Horrocks, W. D., Jr.; Sudnick, D. R. *J. Am. Chem. Soc.* **1979**, *101*, 334–340. (b) Horrocks, W. D., Jr.; Sudnick, D. R. *Acc. Chem. Res.* **1981**, *14*, 384–392.
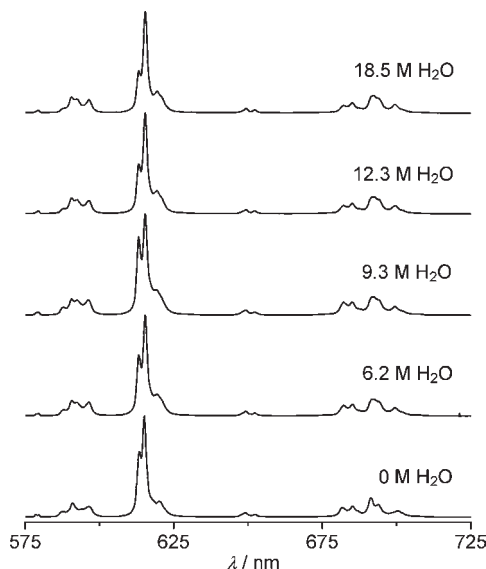
Figure 7. Emission spectra (λ_{ex} = 370 nm) recorded for [Eu(**5b**)₂-(CF₃SO₃)](CF₃SO₃)₂ 1 mM in degassed CH₃CN containing various amounts of water.

Changes for all the Eu(III)-centered emissions were observed, but the $^5D_0 \rightarrow{}^7F_2$ transition shows the most profound variation. The $^5D_0 \rightarrow{}^7F_2$ to $^5D_0 \rightarrow{}^7F_1$ intensity ratio decreases from 3.9 for the water-free sample to 3.3 for the sample containing 18.5 M of water, reflecting some changes in the coordination environment. On the other hand, the overall quantum yield Q_{Eu}^{L} is relatively insensitive to the change in solvent composition, varying from 0.63(5) to 0.56(5) %, while the sensitization efficiency remains the same within experimental error.

In this study we have examined the coordination of several quaterpyridine derivatives with Eu(III). Although the parent polypyridine does not bind in a well organized fashion, the replacement of bpy subunits with the more conformationally restricted phen moiety increases the ligand preorganization and leads to a 2:1 ligand−metal complex with the ninth coordination site occupied by water or triflate. The conformation of the bridged biphen ligands modulates their electronic absorption properties which in turn is reflected by the emission properties of the Eu(III) complexes. The highly preorganized nature of these ligands[18] makes them unusually resistant to replacement by added water and the consequential luminescence quenching which such hydration ordinarily would cause.

Experimental Section

^{1}H NMR spectra were obtained at 300 MHz on a General Electric QE-300 spectrometer. Chemical shifts are reported in parts per million relative to tetramethylsilane, SiMe₄. Absorption spectra were recorded with a Varian Cary-50 Bio spectrophotometer. All spectra were corrected for the background spectrum of the solvent. MALDI-TOF mass spectra were obtained on an Applied Biosystems Voyager DE STR-4160 spectrometer using α-cyano-4-hydroxycinnamic acid as the matrix and CH₃CN as the solvent except for the complex of **6** where a mixture of CHCl₃ and MeOH was used. The ligands **4**,[12a] **5a-d**,[13,19] and **6**[12b] were prepared according to

published procedures as was the complex [Eu(tpy)₃](ClO₄)₃.[3] Eu(CF₃SO₃)₃ and Eu(ClO₄)₃·6H₂O were purchased from Aldrich and Johnson Matthey Inc., respectively. Elemental analyses were carried out by QTI, P.O. Box 470, Whitehouse, NJ 08888−0470.

Luminescence spectra were recorded either with a Perkin-Elmer LS-50B luminescence spectrometer or a Fluorolog FL3−22 spectrofluorimeter from Horiba-Jobin-Yvon Ltd. on well ground solid samples or solutions in acetonitrile in special 2.4 mm i.d. quartz capillaries. All excitation and luminescence spectra were corrected for the instrumental functions. Quantum yields were determined under ligand excitation (330−370 nm) and using an absolute method based on a specially modified integration sphere from GigaHertz Optik in Zenith Teflon with a 2 in. diameter.[20]

Lifetimes of the Eu($^5D_0$) level were measured upon ligand excitation at 355 nm provided by a Quantum Brillant Nd:YAG laser equipped with frequency tripler and monitoring the $^5D_0 \rightarrow{}^7F_2$ transition; luminescence decays were analyzed with Origin. Lifetime values are averages of at least three independent experiments. Excitation spectra were recorded upon monitoring the $^5D_0 \rightarrow{}^7F_2$ transition. All measurements have been carried out at room temperature (295 K).

[Eu(4)₂(H₂O)](ClO₄)₃. A solution of Eu(ClO₄)₃·6H₂O (56 mg, 0.10 mmol) in EtOH (3 mL) was added dropwise to a refluxing solution of **4** (83.5 mg, 0.25 mmol) in EtOH (7 mL). Reflux was continued overnight under Ar. After cooling, the precipitate was collected and washed with EtOH to afford a white powder (116 mg, 100%): ^{1}H NMR (CD₃CN) δ 7.74 (d, J = 8.1 Hz, 4H), 7.26 (t, J = 7.8 Hz, 4H), 6.64 (broad, 4H), 5.80 (broad, 4H), 5.57 (m, 4H), 5.14 (d, J = 7.5 Hz, 4H), 4.91 (m, 4H); MS m/z 863.356 [M−2ClO₄−H₂O+CH₃CN+H]⁺, 841.319 [M−3ClO₄+2H]⁺, 774.252 [M-2ClO₄−(**4**)+(matrix-H)]⁺, 920.380 [M−2ClO₄−H₂O]⁺. Anal. Calcd for C₄₄H₃₀Cl₃EuN₈O₁₃·H₂O: C, 45.75; H, 2.79; N, 9.70. Found: C, 46.09; H, 2.80; N, 9.58. A crystal suitable for X-ray analysis was obtained by slow evaporation of an acetonitrile solution.

[Eu(4)₂(CF₃SO₃)](CF₃SO₃)₂. A solution of Eu(CF₃SO₃)₃ (15 mg, 0.025 mmol) and **4** (16.7 mg, 0.050 mmol) in EtOH (15 mL) was refluxed for 16 h. The solvent was evaporated, and the residue, dissolved in a small amount of CH₃CN, was purified on a short alumina column eluting with CH₃CN to give [Eu(**4**)₂(CF₃SO₃)](CF₃SO₃)₂ as a light yellow solid (22 mg, 69%): ^{1}H NMR (CD₃CN) δ 8.17 (broad, 4H), 7.35 (broad, 4H), 6.85 (broad, 4H), 5.42 (broad, 4H), 4.88 (broad, 4H), 4.62 (broad, 4H), 1.25 (broad, 4H). ^{1}H NMR (CD₃COCD₃) δ 8.52 (broad, 4H), 7.62 (broad, 4H), 6.94 (broad, 4H), 5.57 (broad, 4H), 5.29 (broad, 4H), 4.93 (broad, 4H), 1.27 (broad, 4H); MS m/z 822.369 [M−3CF₃SO₃]⁺, 783.210 [M−CF₃SO₃-(**4**)]⁺, 636.261 [M−2CF₃SO−(**4**)]⁺, 335.360 [**4**+H]⁺. Anal. Calcd for C₄₇H₂₈EuF₉N₈O₉S₃: C, 44.52; H, 2.23; N, 8.84. Found: C, 44.90; H, 2.63; N, 8.65.

[Eu(5a)₂(CF₃SO₃)](CF₃SO₃)₂. A solution of Eu(CF₃SO₃)₃ (60 mg, 0.10 mmol) in MeOH (3 mL) was added dropwise to a refluxing solution of **5a** (90 mg, 0.25 mmol) in MeOH (10 mL). The resulting mixture was heated at reflux overnight under Ar. After cooling, the solid was filtered and washed with CH₃CN. The filtrate was then evaporated, and the residue was dissolved in CH₃CN. Insoluble material was again filtered and washed with CH₃CN. Evaporation of the filtrate yielded [Eu(**5a**)₂-(CF₃SO₃)](CF₃SO₃)₂ as a light beige powder (114 mg, 87%): ^{1}H NMR (CD₃CN) δ 7.61 (broad, 4H), 7.58 (broad, 4H), 6.69 (d, J = 7.5 Hz, 4H), 6.58 (broad, 4H), 5.50 (broad, 4H), 4.53 (d, J = 8.7 Hz, 4H), 3.27 (d, J = 5.7 Hz, 4H); MS m/z 659.915 [M−2CF₃SO₃−(**5a**)]⁺, 359.176 [**5a**+H]⁺. Anal. Calcd

(18) Cockrell, G. M.; Zhang, G.; VanDerveer, D. G.; Thummel, R. P.; Hancock, R. D. *J. Am. Chem. Soc.* **2008**, *130*, 1420–1430.

(19) Hu, Y.-Z.; Xiang, Q.; Thummel, R. P. *Inorg. Chem.* **2002**, *41*, 3423–3428.

(20) Aebischer, A.; Gumy, F.; Bünzli, J.-C. G. *Phys. Chem. Chem. Phys.* **2009**, *11*, 1346–1353.

for $C_{51}H_{28}N_8O_9F_9S_3Eu \cdot 4H_2O$: C, 44.13; H, 2.61; N, 8.07. Found: C, 44.14; H, 2.19; N, 7.97.

[Eu(5b)$_2$(CF$_3$SO$_3$)](CF$_3$SO$_3$)$_2$. Following the procedure described for [Eu(5a)$_2$(CF$_3$SO$_3$)](CF$_3$SO$_3$)$_2$, **5b** (96 mg, 0.25 mmol) was treated with Eu(CF$_3$SO$_3$)$_3$ (60 mg, 0.10 mmol) to afford [Eu(5b)$_2$(CF$_3$SO$_3$)](CF$_3$SO$_3$)$_2$ as yellow flakes (122 mg, 89%): ^{1}H NMR (CD$_3$CN) δ 7.72 (broad, 4H), 7.10 (broad, 4H), 6.73 (broad, 4H), 6.38 (broad, 4H), 5.58 (broad, 4H), 2.41−2.01 (m, 12H); MS m/z 1069.954 [M−2CF$_3$SO$_3$]$^+$, 921.091 [M−3-CF$_3$SO$_3$]$^+$, 686.068 [M−2CF$_3$SO$_3$−(5b)]$^+$, 385.258 [5b+H]$^+$. Anal. Calcd for $C_{55}H_{32}EuF_9N_8O_9S_3 \cdot H_2O$: C, 47.66; H, 2.47; N, 8.08. Found: C, 47.42; H, 2.16; N, 7.95. A light yellow crystal suitable for X-ray analysis was obtained by slow evaporation of an acetonitrile solution.

[Eu(5c)$_2$(CF$_3$SO$_3$)](CF$_3$SO$_3$)$_2$. Following the procedure described for [Eu(5a)$_2$(CF$_3$SO$_3$)](CF$_3$SO$_3$)$_2$, **5c** (99.5 mg, 0.25 mmol) was treated with Eu(CF$_3$SO$_3$)$_3$ (60 mg, 0.10 mmol) to afford [Eu(5c)$_2$(CF$_3$SO$_3$)](CF$_3$SO$_3$)$_2$ as yellow flakes (122 mg, 87%): ^{1}H NMR (CD$_3$CN) δ 7.92 (broad, 4H), 7.51 (broad, 4H), 6.74 (broad, 8H), 5.08 (broad, 4H), 2.36 (m, 8H), 2.04 (broad, 8H); MS m/z 1098.168 [M−2CF$_3$SO$_3$]$^+$, 700.173 [M−2CF$_3$SO$_3$−(5c)]$^+$, 399.346 [5c+H]$^+$. Anal. Calcd for $C_{57}H_{36}EuF_9N_8O_9S_3$: C, 49.04; H, 2.60; N, 8.03. Found: C, 48.85; H, 2.44; N, 7.81.

[Eu(5d)$_2$(CF$_3$SO$_3$)](CF$_3$SO$_3$)$_2$. Following the procedure described for [Eu(5a)$_2$(CF$_3$SO$_3$)](CF$_3$SO$_3$)$_2$, **5d** (82 mg, 0.20 mmol) was treated with Eu(CF$_3$SO$_3$)$_3$ (60 mg, 0.10 mmol) to afford [Eu(5d)$_2$(CF$_3$SO$_3$)](CF$_3$SO$_3$)$_2$ as a yellow solid (106 mg, 74%): ^{1}H NMR (CD$_3$CN) δ 8.18 (broad, 4H), 7.72 (broad, 4H), 6.91 (broad, 8H), 5.30 (broad, 4H), 2.08 (m, 8H), 1.74−1.10 (m, 12H); MS m/z 1125.869 [M−2CF$_3$SO$_3$]$^+$, 713.909 [M−2CF$_3$SO$_3$−(5d)]$^+$, 413.234 [5d+H]$^+$. Anal. Calcd for $C_{59}H_{40}EuF_9N_8O_9S_3 \cdot 5H_2O$: C, 46.80; H, 3.33; N, 7.40. Found: C, 46.79; H, 2.70; N, 7.25.

[Eu(6)$_2$(CF$_3$SO$_3$)](CF$_3$SO$_3$)$_2$. A solution of Eu(CF$_3$SO$_3$)$_3$ (60 mg, 0.10 mmol) in MeOH (5 mL) was added dropwise to a refluxing suspension of **6** (109 mg, 0.25 mmol) in MeOH (10 mL) under Ar. Reflux was continued overnight. After cooling, the precipitate was collected as a beige powder (120 mg, 81%): ^{1}H NMR (CD$_3$CN) δ 9.72 (broad, 4H), 8.82 (broad, 4H), 8.39 (broad, 4H), 6.82 (broad, 8H), 5.6 (broad, 4H), 5.42 (broad, 4H), 5.2−4.6 (broad, 4H); MS m/z 965.178 [M−2CF$_3$SO$_3$−(6)+(matrix-H)+K]$^+$, 926.105 [M−2CF$_3$SO$_3$−(6)+(matrix-H)]$^+$, 887.077 [M−CF$_3$SO$_3$−(6)], 738.129 [M−2CF$_3$SO$_3$−(6)], 437.326 [6+H]$^+$. Anal. Calcd for $C_{59}H_{32}EuF_9N_{12}O_9S_3$: C, 48.14; H, 2.19; N, 11.42. Found: C, 48.79; H, 2.52; N, 11.59.

X-ray Analyses. **[Eu(4)$_2$(H$_2$O)](ClO$_4$)$_3$.** A colorless crystal of [Eu(4)$_2$(H$_2$O)](ClO$_4$)$_3 \cdot 1.5H_2O \cdot 1.5CH_3CN$, with the dimensions of $0.35 \times 0.25 \times 0.10$ mm^3, was measured with a Siemens SMART platform diffractometer equipped with a 1K CCD area detector. A hemisphere of data (1271 frames at 5 cm detector distance) was collected using a narrow-frame method with scan widths of $0.30°$ in ω and an exposure time of 30 s/frame. The first 50 frames were remeasured at the end of data collection to monitor instrument and crystal stability, and the maximum correction on I was < 1%. The data were integrated using the Siemens SAINT program, with the intensities corrected for Lorentz factor, polarization, air absorption, and absorption because of variation in the path length through the detector faceplate. A ψ scan absorption correction was applied based on the entire data set. Redundant reflections were averaged. Final cell constants were refined using 5584 reflections having $I > 10\sigma(I)$, and these, along with other information pertinent to data

collection and refinement, are listed in Supporting Information, Table S1. The Laue symmetry was determined to be −1, and the space group was shown to be either $P1$ or $P\bar{1}$. The asymmetric unit consists of two independent cations, six anions, three waters of solvation, and three molecules of acetonitrile. Four of the perchlorate anions were found to be disordered over two slightly different orientations, and this was treated using ideal rigid body models having partial occupancies. One of the acetonitrile molecules is also disordered, and was treated similarly. On the basis of isotropic temperature factors, it was determined that two of the solvent water sites are not fully occupied. Presumably this was caused by solvent loss during handling, and so for all calculations 100% occupancy was assumed. No attempt was made to locate or include hydrogen atoms on the coordinated water, solvent water, or acetonitrile molecules.

[Eu(5b)$_2$(CF$_3$SO$_3$)](CF$_3$SO$_3$)$_2$. A yellow flat block of [Eu(5b)$_2$(CF$_3$SO$_3$)](CF$_3$SO$_3$)$_2 \cdot 4CH_3CN$, with the dimensions of $0.45 \times 0.30 \times 0.20$ mm^3, was measured with a Siemens SMART platform diffractometer equipped with a 4K CCD APEX II detector. A hemisphere of data (1271 frames at 6 cm detector distance) was collected using a narrow-frame algorithm with scan widths of $0.30°$ in ω and an exposure time of 25 s/frame. The data were integrated using the Bruker-Nonius SAINT program, with the intensities corrected for Lorentz factor, polarization, air absorption, and absorption because of variation in the path length through the detector faceplate. A ψ scan absorption correction was applied based on the entire data set. Redundant reflections were averaged. Final cell constants were refined using 8176 reflections having $I > 10\sigma(I)$, and these, along with other information pertinent to data collection and refinement, are listed in Supporting Information, Table S1. The Laue symmetry was determined to be −1, and the space group was shown to be either $P1$ or $P\bar{1}$. The asymmetric unit consists of one Eu complex, two triflate anions, and four acetonitrile solvent molecules. The triflate attached to Eu is disordered 75:25, and one of the two other triflates (S3) is disordered 60:40. All but the 75% orientation were modeled as ideal rigid bodies based on the geometry of the S2 ordered molecule. Three of the four acetonitrile solvent molecules seem to have some minor disorder; however, they were refined allowing anisotropic displacement parameters to account for the slight positional variations. The fourth acetonitrile is significantly disordered, and only the two main orientations comprising 80% total occupancy could be located and refined. However, for all calculations it is assumed that this site is fully occupied and that some solvent was lost during sample handling.

Supporting Information Available: X-ray crystallographic data for [Eu(4)$_2$(H$_2$O)](ClO$_4$)$_3$ and [Eu(5b)$_2$(CF$_3$SO$_3$)](CF$_3$SO$_3$)$_2$ (CIF files and Table S1); integral intensities in the solid state (Table S2) and in CH$_3$CN solution (Table S3); excitation spectra (Figure S1) and emission spectra (Figure S2) for solid state samples. This material is available free of charge via the Internet at http://pubs.acs.org.